A PLANAR ANTENNA ARRAY MANUFACTURED FROM CARBON FIBRE REINFORCED PLASTIC

Paul J. Callus*, Kelvin J. Nicholson*, Alexe Bojovschi, Kamran Ghorbani**, William Baron*** and James Tuss*****
***Defence Science and Technology Organisation (DSTO), Air Vehicles Division, 506 Lorimer Street, Fishermans Bend, Victoria, AUSTRALIA**
****RMIT University, School of Electrical and Computer Engineering, Swanston Street, Melbourne, Victoria, AUSTRALIA**
*****Air Force Research Laboratory, Air Vehicles Directorate, Wright Patterson Air Force Base, Dayton, Ohio, USA**
paul.callus@dsto.defence.gov.au

Keywords: *planar antenna array, carbon fibre reinforced plastic*

Abstract

A structural sandwich panel that also acted as a planar antenna array was designed, manufactured and tested. The flat 340 mm x 340 mm sandwich panel was manufactured from IM7/977-3 carbon fibre reinforced plastic. The skins in this panel were separated by parallel blades, creating tubes with a 22.9 mm x 10.2 mm cross-section. This matches that of WR90 waveguides used for the transmission of X-band (8-12 GHz) radiation. Ten longitudinal slots were cut through the outer skin and into each of the ten central tubes, and custom radiofrequency feeds and electrical shorts fitted to the ends of these tubes. 10 GHz radiation was fed into the feeds and the radiofrequency response measured. The scattering parameters and antenna pattern matched that predicted by radiofrequency simulation and demonstrated that a structural panel could also behave as a planar slotted waveguide antenna array.

1 Introduction

1.1 Antennas

The capability to transmit and receive radiofrequency (RF) signals is a critical requirement for many modern military platforms. Antennas are fundamental to this because they transition the RF signals from/to the internal systems to/from free space.

Platforms can contain many tens, and even hundreds, of antennas. For example fighter aircraft and Guided Missile Destroyers have in the order of 80 antennas while nuclear aircraft carriers have nearly 150 [1]. The conventional approach to installing these antennas is that each is supplied as a separate part that is fastened to the platform exterior or, in some cases, under a radome.

The redundancy inherent in this approach increases weight and volume, thereby potentially degrading the platform's performance (speed, range, endurance, payload). This, coupled with considerations such as signal masking and mutual interference, constrains the size and location of antennas.

The utility of some RF systems could be enhanced by increasing the size of:

- Individual antenna elements.
  Operating frequency is inversely proportional to element size and the detection capability of sensing systems can be enhanced by operation at different frequencies.
- Antenna arrays.
  Beam width is inversely proportional to array size. Precision sensing, secure communications and satellite communications are enhanced by narrower beams, which can be achieved through larger arrays.

1.2 Slotted Waveguide Antenna Stiffened Structure (SWASS)

1.2.1 Concept

The aim of Conformal Load-bearing Antenna Structure (CLAS) is to expand the range of allowable antenna/array size and location by integrating the antenna with the platform structure [2, 3]. This would allow antenna elements and arrays to be disproportionately larger than their conventional counterparts, thereby realizing the RF system enhancements described in Section 1.1.

Slotted Waveguide Antenna Stiffened Structure (SWASS) is a form of CLAS where the hollow, top-hat cross-section, stiffeners bonded to the back of thin skins, or blade stiffeners in sandwich panels, serve the dual purpose of acting as structural stiffeners and as RF waveguides. Slots cut through the outer skin and into the stiffener/waveguides create slotted waveguide antennas. The slots are then filled with a RF transparent dielectric to restore the outer mould line. Fig. 1 shows one potential SWASS configuration.

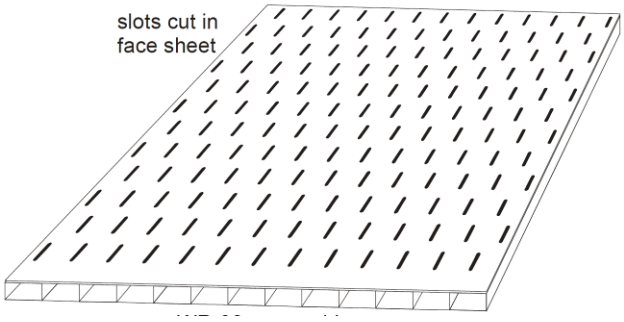

Fig. 1. Schematic of a possible SWASS configuration, a blade stiffened sandwich panel with an array of longitudinal slots cut through the broad-wall of the stiffener waveguides.

1.2.2 Previous work

It has been shown previously that:

- RF energy can be transmitted through waveguides manufactured from commercially available aerospace grade carbon fibre reinforced plastic (CFRP) although this energy is attenuated at a relatively high 0.05 dB/cm [3].
- the antenna patterns from single and multi-slot antenna arrays in single CFRP waveguides are similar in shape, but lower in gain, to those from the same slot geometry in copper waveguides [4, 5], and
- RF energy can be fed into CFRP waveguides using a custom loop-type, end-launch, RF feed [5].

1.2.3 Current work

This paper summarises the RF design, manufacture and RF testing of a generic SWASS at the structural element level, specifically a blade-stiffened sandwich panel containing a 10 slot x 10 slot planar antenna array.

2 RF Design

The RF analysis and design were conducted using the Finite Element Method (FEM) implemented in ANSYS Corporation's High Frequency Structural Simulator (HFSS) [5] and the Method of Moments (MoM) implemented in Electromagnetic Software and Systems' (EMSS) FEldberechnung für Körper mit beliebiger Oberfläche (FEKO) [6].

2.1 RF Propagation in CFRP Waveguides

In a typical aerospace grade CFRP laminate with a fibre content of 60% by volume, the 5-7 μm fibre diameter, moderately conductive, carbon fibres are separated by 1-3 μm. This volume is filled with non-conductive polymer resin. CFRP therefore acts as a moderate conductor in the direction of the fibres and a lossy dielectric perpendicular (both in-plane and out-of-plane) to the fibres. The RF conductivity of CFRP laminates is highly dependent on ply stacking sequence and accounting for this is an important part of the RF design process for SWASS antennas.

A model of the anisotropic RF conductivity of CFRP was devised, validated experimentally then implemented in HFSS using a tensorial formulation [7].

FEM models of CFRP waveguides with the same 22.86 mm x 10.16 mm internal cross-

section as rigid rectangular WR90 waveguides used for the transmission of X-band (8 – 12 GHz) radiation, were created in HFSS. The waveguide walls were modeled as four ply CFRP laminates with ply stacking sequences of $[0\ 90]_s$, $[90\ 0]_s$ and $[\pm 45]_s$. Fig. 2 is a schematic of a four ply $[90\ 0]_s$ CFRP laminate. In this work the 0° fibre direction was parallel to the longitudinal axis of the waveguide.

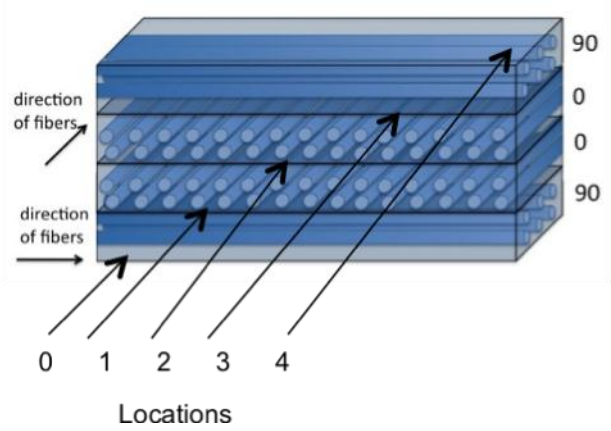

Fig. 2. A section of the model used to simulate RF attenuation in CFRP waveguides showing the waveguide wall with a $[90\ 0]_s$ ply stacking sequence and the through-thickness locations (numbered) where current density was predicted.

Analysis of the current densities and Poynting vector [7] was conducted in order to quantify the attenuation of RF waves in CFRP waveguides. The vector current density on the inner walls of the waveguides ($\vec{J}$) is proportional to the magnetic field vector ($\vec{H}$), specifically $\vec{J} = \hat{n} \times \vec{H}$. The current density on the broad-wall can be calculated by computing the components:

$$J_x = -j \frac{\beta_x}{\omega \mu} E_0 \cos(\beta_x x) e^{-j\beta_z z} \qquad (1)$$

and

$$J_z = -\frac{\beta_z}{\omega \mu} E_0 \sin(\beta_x x) e^{-j\beta_z z} \qquad (2)$$

while the current density on the narrow-wall is obtained from:

$$J_y = -j \frac{\beta_x}{\omega \mu} E_0 e^{-j\beta_z z} \qquad (3)$$

where subscripts *x*, *y* and *z* denote the Cartesian directions.

It should be noted that current density on the top wall of the waveguide is the reverse of that on the bottom, $\vec{J}^{bottom} = -\vec{J}^{top}$.

The predicted current densities at 10 GHz on the waveguide broad- and narrow-walls are, shown in Figs 3 and 4 respectively. The current density decreases from the inner surface of the waveguide wall (Fig. 2, Location 0) to the outer surface (Fig. 2, Location 4) exponentially.

At 10 GHz it was found that the $[0\ 90]_s$ ply stacking sequence gave the lowest attenuation. This ply stacking sequence was therefore selected for the waveguide walls in the SWASS panel.

2.2 RF Feed and CFRP End-Short

It was necessary to feed RF waves into the CFRP waveguides if they were to act as antennas. Traditional coaxial-to-waveguide transitions were too large for the ten adjacent waveguides in the panel so a custom, loop-type, end-launch, RF feed was developed [5].

Various loop transitions [4-6] and stepped or linearly tapered ridge waveguide sections [7, 8] were considered. However, these feeds required grounding by direct electrical connection to the waveguide wall. It is not practical to do this for the CFRP waveguides because this would require the 1-3 μm resin skin surrounding each fibre to be abraded off and an electrical connection made with these fibres.

A loop-type, end-launch, RF feed for CFRP waveguides had been devised previously and designed to resonate at 9.375 GHz. [5]. This feed was adapted to make it more appropriate for incorporation into a CFRP aircraft structure and to resonate at 10 GHz.

The new feed consisted of a CFRP tube supporting a loop-type antenna fed with a standard SMA connector. A model and photograph of the feed is shown in Fig. 5.

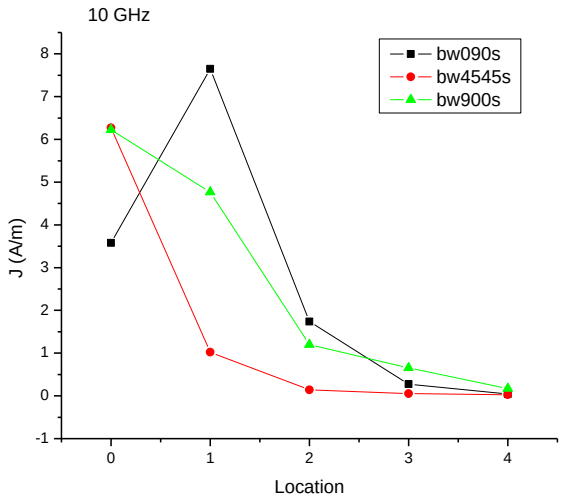

Fig. 3. The predicted effect of through-thickness location (refer to Fig. 2 for locations) and ply stacking sequence on the current density in the waveguide broad-wall (bw).

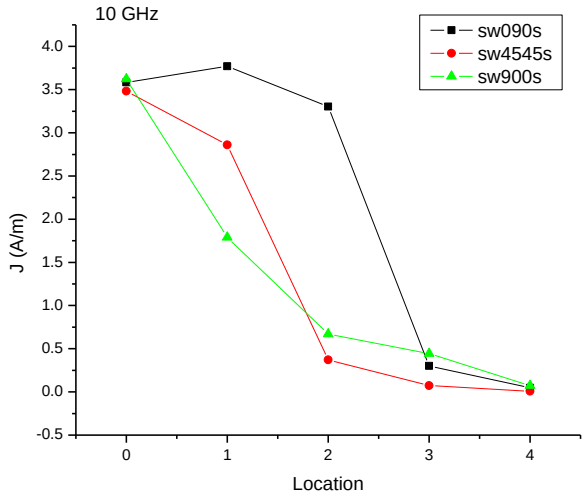

Fig. 4. The predicted effect of through-thickness location (refer to Fig. 2 for locations) and ply stacking sequence on the current density in the waveguide narrow-wall (sw).

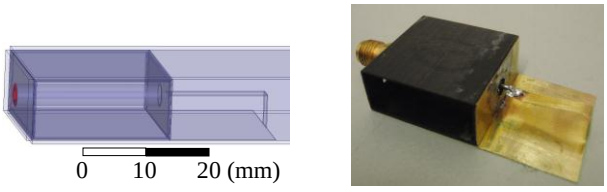

(a) (b)

Fig. 5. (a) Model and (b) photograph of the loop-type, end-launch, RF feed.

The optimal dimensions for the RF feed were acquired using simulation. A HFSS model was created of the RF feed, a 30 cm section of CFRP WR90 waveguide with a $[0\ 90]_s$ ply stacking sequence, and an end-short at the far-end of the waveguide.

The end-short reflected the RF waves back into the waveguide, creating a standing wave. In resonant slot antennas such as that developed here, the end-short would be placed at a quarter of a guided wavelength ($\lambda_g/4$) from the centre of the last slot so that the peak of the standing wave was centred on the slot. The guided wavelength (λ_g) is the wavelength in the waveguide and is longer than the free-space wavelength (λ_0) at the same frequency. The remaining slots would be separated by $\lambda_g/2$, again so they too would be centered on the peaks of this standing wave.

In this work the end-short consisted of a CFRP tube, placed side-ways in the CFRP waveguide. The dimensions and ply stacking sequence of the end-short were the same as that of the tubes in the RF feed.

The effective conductivity and permittivity tensors for the broad-walls and narrow-walls of the CFRP tubes in the RF feed and the end-short are shown respectively in Equations 4 and 5.

$$\begin{aligned} \mathbf{C}90b &= (c\ 0\ 0) * I \\ \mathbf{C}90a &= (c\ 0\ 0) * I \\ \mathbf{C}0b &= (0\ 0\ c) * I \\ \mathbf{C}0a &= (0\ c\ 0) * I \end{aligned} \tag{4}$$

$$\begin{aligned} \mathbf{E}90b &= (0\ e\ e) * I \\ \mathbf{E}90a &= (0\ e\ e) * I \\ \mathbf{E}0b &= (e\ e\ 0) * I \\ \mathbf{E}0a &= (e\ 0\ e) * I \end{aligned} \tag{5}$$

where I is the identity matrix. The *x*, *y* and *z* components of the effective conductivity (c) and permittivity (e) are given elsewhere [7, 14]. The tensorial description for the broad- and short-wall of the waveguides is given in [7].

Successive simulation runs were conducted with the dimensions of the RF feed varied slightly for each run. The design dimensions were those that were predicted to give the minimum return loss (S11) at 10 GHz.

The simulated effect of frequency on S-parameters of the RF feed installed in aluminium alloy (Al) and CFRP waveguides are shown in Fig. 6. The dip in the S11 return loss at 10 GHz indicates the operating frequency of this feed. The S21 insertion loss for the feed in the CFRP waveguide was predicted to be 1.75 dB lower than that in the Al waveguide. This was caused by attenuation loss in the CFRP waveguides [7] which was accounted for in the simulation of the feed system.

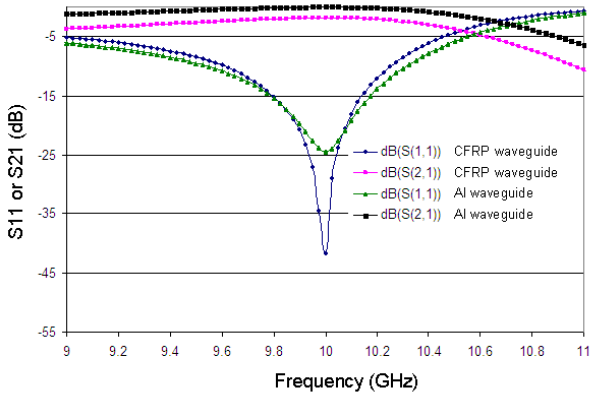

Fig. 6. Simulated S-parameters for the loop-type, end-launch, RF feed in 30 cm long waveguides manufactured from aluminium alloy (Al) and $[90\ 0]_s$ CFRP.

2.3 1 x 10 Sub-Array Design

A resonant, ten element, slotted waveguide antenna array (1 x 10 sub-array) with longitudinal slots in the broad-wall and uniform amplitude illumination was designed. The nominal slot dimensions were: 14.47 mm long, 1.60 mm wide, 0.8 mm tip-radius, 2.50 mm offset from the centre-line, and 15.00 mm centre-to-centre separation. A model of the 1 x 10 sub-array with RF feed and CFRP end-short is shown in Fig. 7.

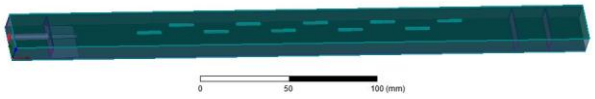

Fig. 7. A model of the 1 x 10 sub-array including RF feed and CFRP end-short.

The resonant length of the slots was determined numerically. This approach induced some error because it assumed that the waveguide wall was a perfect electrical conductor, however the magnitude of this error was not expected to be significant because the dominant factor, the effect of waveguide wall thickness, was accounted for [15].

2.4 10 x 10 Slot Array Design

Considerable computing resources would be required to FEM mesh of the 10 x 10 slot array with sufficient detail for a meaningful MoM solution. Thus in the simulations done in this work the RF feed and CFRP end-short were replaced, respectively, with waveguide ports and aluminium end-shorts. The waveguide material was kept as CFRP.

The model of the planar array together with the predicted intensity of electric field across the slots at the resonant frequency of 10 GHz is shown in Fig. 8. The field strength in the slots was predicted to be 1,000-5,000 V/m.

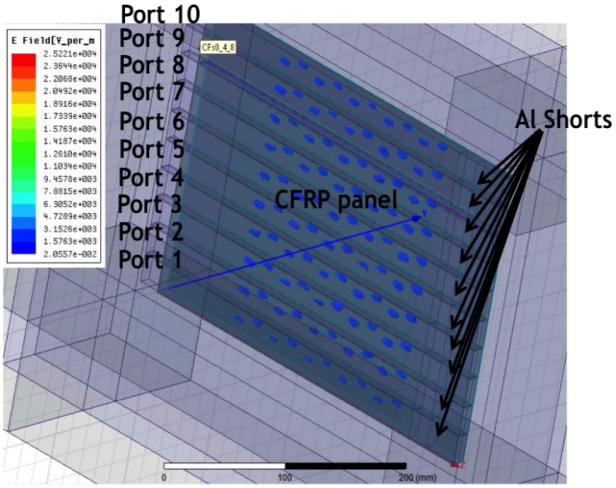

Fig. 8. The 10 x 10 slot planar antenna array, waveguide port and end-short model and the predicted E-fields.

Fig. 9 shows the simulated antenna patterns for the 1 x 10 sub-arrays while Fig. 10 shows the simulated three dimensional pattern for the entire 10 x 10 slot array. The peak gain for the former was predicted to be 12.6 dB and the latter 23.1 dB.

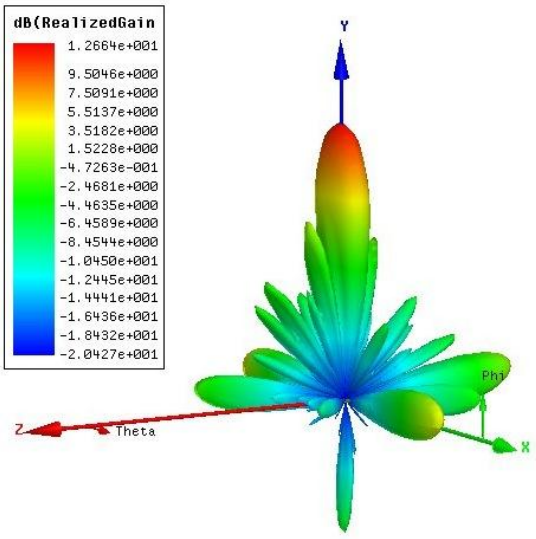

(a)

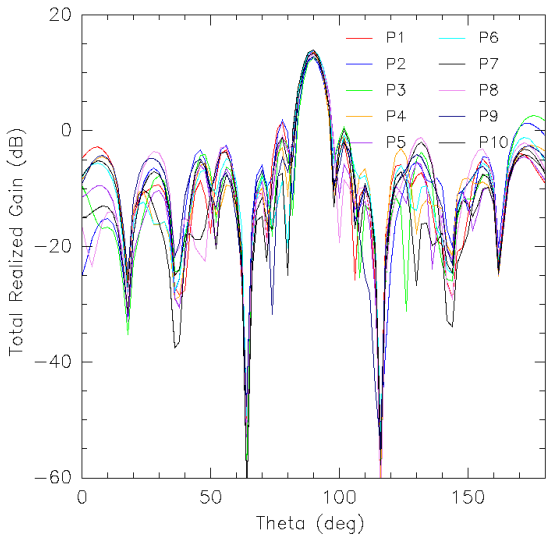

(b)

Fig. 9. Simulated realized gain at 10 GHz of the (a) 1 x 10 sub-array at Port 2 and (b) each of the 1 x 10 sub-arrays.

3 Manufacture

3.1 Panel

Fifteen 400 mm long aluminium mandrels were; coated with release film, wrapped with four 350 mm long plies of IM7/977-3 unidirectional prepreg tape in a $[0\ 90]_s$ ply stacking sequence, then vacuum debulked. The cross-section of the mandrels and release film was such that after cure the inner dimension of the CFRP waveguides would be close to the 22.86 mm x 10.16 mm of WR90 waveguides.

Two 350 mm x 350 mm flat skins of IM7/977-3 unidirectional prepreg tape, with a $[0\ 90]_s$ ply stacking sequence, were laid up and vacuum debulked.

One of the skins was positioned on the bed of a SWASS Flat Panel Tool. The wrapped and debulked mandrels were then located on the skin as shown in Fig. 11. Once all mandrels had been stacked the outer skin was located over the assembly and the tool vacuum bagged. The part was autoclave cured at 177 °C and 586 kPa for 6 hours in accordance with manufacturer's specifications. After curing the panel was released from the tool and trimmed.

The 1 x 10 sub-arrays were machined into each of the central 10 waveguides using a MultiCam M-I Computer Numerically Controlled (CNC) router with a 1.0 mm diameter diamond coated cutter as shown in Fig. 12.

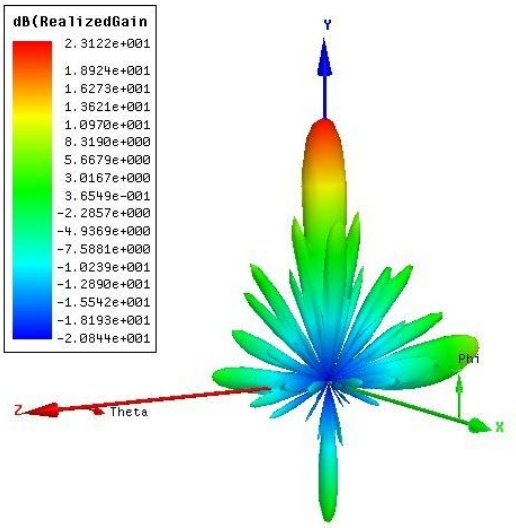

Fig. 10. Simulated (a) three dimensional antenna pattern of the 10 x 10 slot array at 10 GHz.

3.2 RF Feeds and CFRP End-Shorts

A second set of aluminium mandrels were

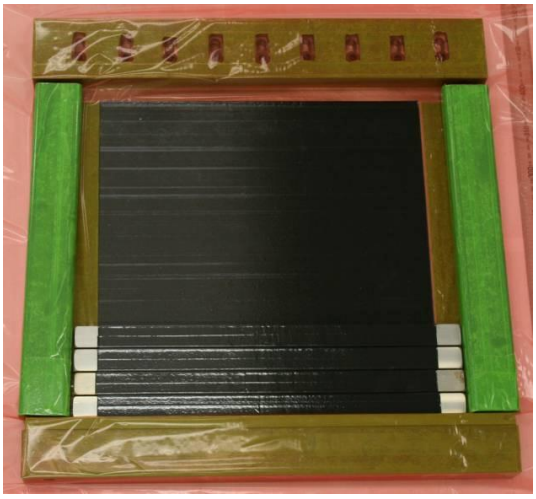

(a)

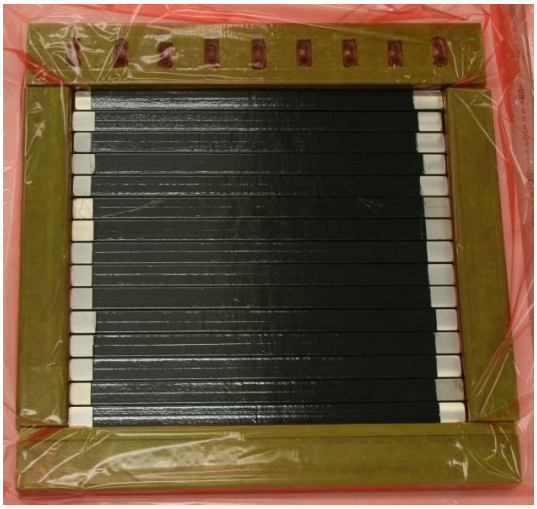

(b)

Fig. 11. Photographs during panel lay-up showing the SWASS Flat Panel Tool with (a) four and (b) all fifteen wrapped mandrels on the skin.

coated with release film, wrapped with four plies of IM7/977-3 unidirectional prepreg tape in a $[0\ 90]_s$ ply stacking sequence, vacuum debulked and autoclave cured in accordance with manufacturer's specifications. The cross-section of these mandrels was such that, after cure, the outer dimension of the CFRP tubes would be approximately 22.8 mm x 10.1 mm. The cured tubes were released then cut into twenty 22.8 mm long pieces.

Ten of these were used as the CFRP end-shorts. In the remaining ten, holes were drilled to accept a SMA connector which allowed

Fig. 12. Photograph showing a slot in the first 1 x 10 array being cut by the CNC router.

connection between the loop-type feed and SMA connector.

The loops were created by cutting pieces of brass shim to shape then folding them. These were then positioned near the CFRP support tube and soldered to the centre conductor and body of the SMA connector. A photograph of a completed RF feed was shown in Fig. 5 (b).

The RF feeds and CFRP end-short were inserted into the central 10 waveguides in the panel.

4 RF Testing

4.1 RF Feed and CFRP End-Short

The RF performance of the RF feed and CFRP end-shorts were measured using the layout shown in Fig. 13. The S-parameters, S21 insertion loss and S11 return loss, were measured over the X-band using a Wiltron 360B Vector Network Analyzer (VNA).

4.2 Antenna Pattern

The antenna pattern of the entire 10 x 10 slot array could not be measured because the size of the available anechoic chamber was not sufficiently large for the measuring horn antenna to be in the far-field of the array.

As an alternative, the radiation pattern of each 1 x 10 sub-arrays was measured in-turn. Array theory was then employed to compute the predicted gain of the 10 x 10 array.

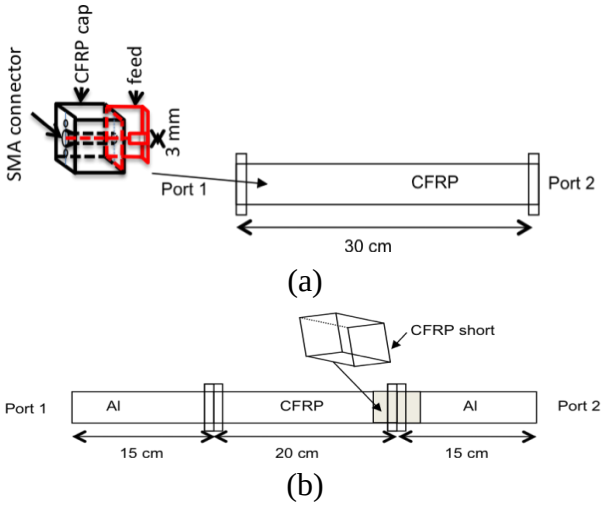

Fig. 13. Layout for characterizing the RF performance of the (a) RF feeds and (b) CFRP end-shorts.

In order to measure the antenna pattern, the entire 10 x 10 slot array was positioned on a turntable at one end of the chamber. A 2-18 GHz horn antenna, with gain of 11.6 dBi at 10 GHz, was located at the opposite end of the chamber. A Wiltron 360B VNA was connected to the horn antenna and, in-turn, each of the 1 x 10 sub-arrays. Antenna pattern were measured as the array was rotated from -180° to +180°.

5 Experimental Results

5.1 Loop-type, end-launch, RF feed

The measured S11 and S21 for the ten RF feeds in a 30 cm length of $[90\ 0]_s$ CFRP waveguide showed that the resonant frequency for these feeds ranged from 10.0 to 10.5 GHz. At the design frequency of 10.0 GHz the return loss for all feeds was below -10 dB, which satisfies the typical return loss criterion for RF feeding. The experimental results of the feeding system in the linear array panel will be reported elsewhere.

5.2 CFRP End-Short

The RF performance of the CFRP end-shorts was shown to be acceptable. Fig. 14 shows that the average S11 return loss at 10 GHz for six CFRP end-shorts was approximately 2.6 dB. Conversely, Fig. 15 shows that transmission through the end-shorts was very low. Although there was some variation, S_{21} for all specimens was below -35 dB at 10 GHz. Both of these results indicate strong reflection, as desired from an end-short.

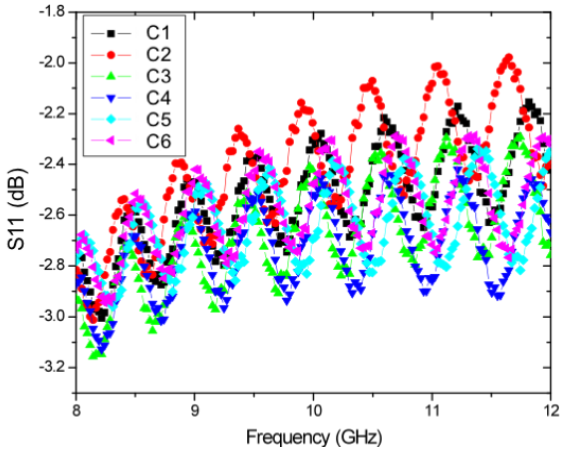

Fig. 14. Measured S11 return loss of six CFRP end-shorts in a 20 cm length of $[0\ 90]_s$ CFRP WR90 waveguide.

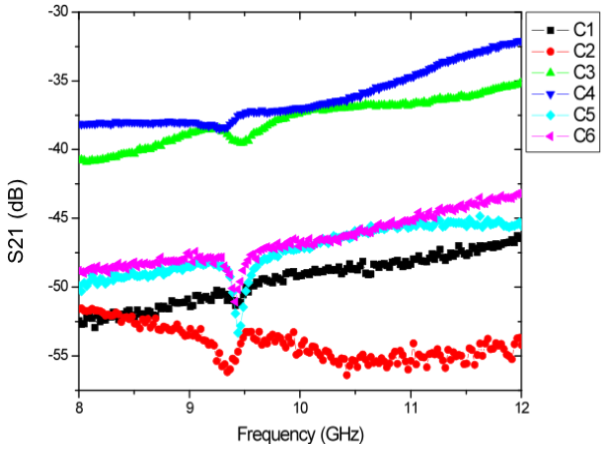

Fig. 15. Measured S21 insertion loss of six CFRP end-shorts in a 20 cm length of $[0\ 90]_s$ CFRP WR90 waveguide.

5.3 Planar Array

5.3.1 1 x 10 sub-arrays

The S11 return loss for each of the 1 x 10 sub-arrays, fitted with the patch-type, end-launch, RF feed and CFRP end-short, was measured and is shown in Fig. 16. For each, S11 dipped well below -10 dB at 10 GHz, indicating resonance at this frequency.

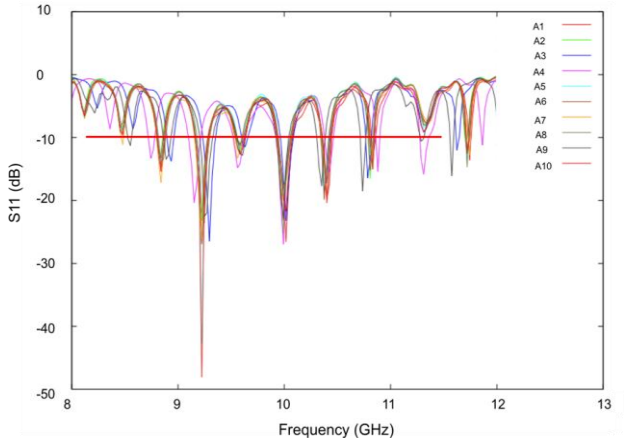

Fig. 16. Measured S11 return loss for each of the 1 x 10 sub-arrays in the 10 x 10 slot planar array.

The antenna pattern from each of the 1 x 10 sub-arrays was measured and showed good agreement with simulation. The average measured gain of each array was approximately 11.6 dB. This is very close to the predicted 12.6 dB when considering that the simulation used an ideal waveguide port and aluminium end-short. Array theory [18] was used to predict the gain of the 10 x 10 slot array on the basis of the array dimensions and the 11.6 dB average measured gain from the 1 x 10 sub-arrays. The array theory prediction was 21.6 dB, which is close to the 23.1 dB predicted in Section 2.4.

6 Future Work

Future work will focus is on developing SWASS designs with:

- representative curvature and edge fastening
- increased bandwidth
- electronic beam steering
- RF transparent windows over the slots.

Each of these features will be designed using the appropriate numerical modeling software (radiofrequency or structural) then demonstrated at the coupon level. The successful techniques will then be brought together and demonstrated at the appropriate structural element/design detail level.

7 Conclusions

This work has demonstrated that a structural panel manufactured from carbon fibre reinforced plastic (CFRP) can also behave as a planar antenna array. A 10 x 10 slot planar antenna array, loop-type, end-launch, RF feed and CFRP end-shorts were designed, manufactured and characterized. The computational and measurement results were in good agreement.

8 Acknowledgements

The work conducted for this study was funded by the Defence Science and Technology Organisation - Corporate Enabling Research Program (DSTO-CERP).

References

[1] Axford, R. A., Jr., Major, R. W., Rockway, J. W., "An Assessment of Multi-function Phased Array Antennas for Modern Military Platforms", *IEEE Proceedings of Phased Array Systems and Technologies*, pp. 365-370, 2003

[2] Lockyer, A. J., Alt, K. H., Coughlin, D. P., Durham, M. D., Kudva, J. N., Goetz, A. C. and Tuss, J., "Design and development of a conformal load-bearing smart skin antenna: overview of the AFRL Smart Skin Structures Technology Demonstration (S^3TD)", *Proceedings of SPIE*, Vol. 3674, pp. 4010-4024, 1999

[3] Callus, P. J., "Novel concepts for conformal load-bearing antenna structure", *Defence Science and Technology Organisation*, Australia, DSTO-TR-2096, Feb. 2008.

[4] Nicholson, K. J. and Callus, P. J., "Antenna patterns from single slots in carbon fibre reinforced plastic waveguides," *Defence Science and Technology Organisation*, Australia, DSTO-TR-2389, August 2010.

[5] Gray, D., Nicholson, K. J., Callus, P. J. and Ghorbani, K., Methods of designing and feeding carbon fibre reinforced plastic slotted waveguide antenna arrays", *DSTO Technical Report*, In review

[6] Ansoft HFSS 13, online resource, 2012.

[7] FEKO, online resource, 2012

[8] Bojovschi A., Nicholson K. J., Galehdar A., Callus P. J. and Ghorbani K., "The role of fibre orientation on the electromagnetic performance of waveguides manufactured from carbon fibre reinforced plastic," *PIER B*, vol. 39, pp 267-280, 2012

[9] Chan K. K., Martin R. and Chadwick K., "A

Broadband End Latinched Coaxial-to-Waveguide Transition for Waveguide Phased Arrays," *Proceedings of IEEE*, pp. 1390-1393, 1998

[10] Deshpande M. D., Das B. N., Sanyal G. S., "Analysis of an End Launcher for an X-Band Rectangular Waveguide," *IEEE Transactions on Microwave Theory and Techniques*, vol. 27, no. 8, pp. 731–735, Aug. 1979

[11] Saad S. M., "A more accurate analysis and design of coaxial-to-rectangular waveguide end launcher," *IEEE Transactions on Microwave Theory and Techniques*, vol. 38, no. 2, pp. 129-134, Feb. 1990

[12] Levy R., Hendrick L. W., "Analysis and synthesis of in-line coaxial-to-waveguide adapters," Proceedings of *IEEE Microwave Symposium*, Seattle, USA, pp. 809-811, Jun 2002

[13] Dix J. C., "Design of waveguide/coaxial transition for the band 2.5-4.1 Gc/s," *Proceedings of The Institute of Electrical Engineers*, vol. 110, no. 2, pp. 253-255, Feb. 1963

[14] Galehdar, A., Rowe W. S. T., Ghorbani K., Callus P. J., John S., and Wang C. H., "The effect of ply orientation on the performance of antennas in or on carbon fibre composites," Progress In Electromagnetics Research, Vol. 116, pp.123-136, 2011.

[15] Josefsson L. G., "Analysis of longitudinal slots in rectangular waveguides", *IEEE Trans. Antennas and Prop.*, Vol. AP-35, No. 12, pp. 1351-1357, 1987

[16] Hexcel Corporation, HexTow IM7 Carbon Fibre Product Data Sheet.

[17] Callus P. J. and Nicholson K. J., "Standard Operating Procedure - Manufacture of Carbon Fibre Reinforced Plastic Waveguides and Slotted Waveguide Antennas," Version 1.0, *Defence Science and Technology Organisation*, Australia, DSTO-TN-0937, June 2011

[18] Balanis, C. A. "Antenna Theory: Analysis and Design", Ed. 3, *John Wiley & Sons*, 2005

Copyright Statement